

EVALUATION OF THE DRIVING FORCE IN FATIGUE CRACK GROWTH, IN PLANE STRAIN AND PLANE STRESS STATE TESTS, UNDER CONSTANT ΔK^*

Julián Andrés Ortiz González¹
Jaime Tupiassú Pinho de Castro²

Abstract

This work presents a series of experiments of Fatigue Crack Growth (FCG), which are intended to provide evidence about the main parameter controlling this phenomenon, whereas still no agreement about this, since the Paris' theory is based on the principle that FCG is controlled by the ΔK and the Elber's theory says that the driving force is ΔK_{eff} . For the development of the experiments, some DC(T) specimens were machined with two different thicknesses: 2 and 30 mm to perform FCG tests in plane stress and plane strain state, respectively. Besides this, all FCG tests were carried out with a constant ΔK e K_{max} , measuring the strain with a Strain-Gage bonded on the back face of the specimen and seven Strain-Gages located on the crack growth path. The data needed to measure the crack opening load, and the ΔK_{eff} , were collected through a program developed in Labview. Finally, the data post-processing was carried out based on the ASTM standards and several articles of recognized authors in this field, in order to compare the two positions with the experimental data, and this way conclude which is the most consistent theory with the observed behavior.

Keywords: Fatigue crack growth; Crack closure; Crack opening load.

¹ B.Sc. in Mechanical Engineering. Mechanical Engineering Department, Pontifical Catholic University of Rio de Janeiro (PUC-Rio), Rio de Janeiro, RJ, Brazil.

² Ph.D. in Mechanical Engineering, Mechanical Engineering Department, Pontifical Catholic University of Rio de Janeiro (PUC-Rio), Rio de Janeiro, RJ, Brazil.

1 INTRODUCTION

Most of the structural components are exposed to a stable and gradual damage process primarily activated by variable loads that generate fatigue, that is crack initiation and/or growth up to an eventual fracture. Therefore, it is almost a general consensus that the fatigue crack initiation is driven by Mises or Tresca strain or stress ranges and maxima. Moreover, many equations were deducted trying to describe the fatigue crack growth (FCG), but there is still no agreement about the driving forces for FCG, focusing the discussion on two basic theories, the Paris' theory (ΔK) and the fatigue crack closure (ΔK_{eff}) [1-2-3-4-5].

1.1 The Paris' Theory

The FCG can be described by the relationship between cyclic crack growth rate da/dN and stress intensity range ΔK . This postulate was made by Paris and Erdogan, in the early 1960s with the Equation 1 [6]:

$$\frac{da}{dN} = A \Delta K^m \quad (1)$$

With A and m as material constants. The equation in a log-log plot gives a linear relation: $\log (da/dN) = \log (A) + m \cdot \log (\Delta K)$ with m as the slope of the linear function. Considering the convention on the existence of three phases of FCG, the Paris' theory only describes the intermediate phase, as shown in **Figure. 1**.

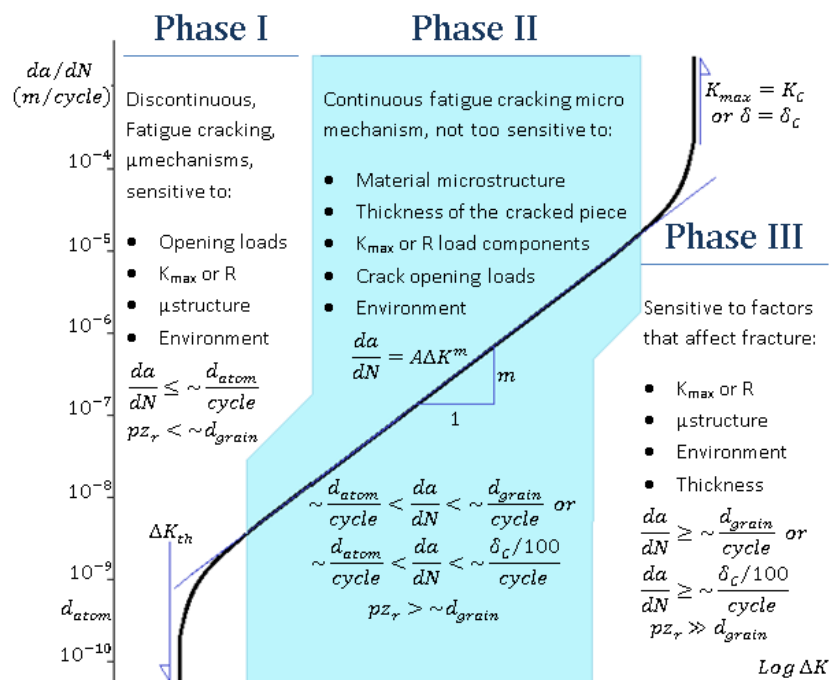


Figure. 1. Typical sigmoidal FCG curve measured at $R=0$, with its 3 characteristic phases (adapted from [1]).

Figure. 1 shows a typical FCG rate, under a fixed R -ratio in metallic alloys, with parameters like atomic diameter d_{atom} , grain size d_{grain} , the reverse plastic zone pz_r , and the critical crack tip opening displacement (CTOD) δ_c . The curve starts when the FCG threshold ΔK_{th} , and finish until the sample fractures when the maximum stress intensity factor value reaches the material toughness, $K_{max} = K_C$.

1.2 Fatigue Crack Closure

Measuring the stiffness of a specimen for FCG during its loading cycle, Elber discovered that the crack only completely opened after reaching an opening load $P_{op} > 0$. He observed that the specimen stiffness decreased as the load was growing between $0 < P < P_{op}$, while for a load $P > P_{op}$ it remained constant, at the stiffness value expected for this case. Crack opening loads P_{op} must be measured at the starting point of the linear stretch on P vs. δ_P (load vs. load application point displacement) curves, as can be seen in **Figure 2** [7].

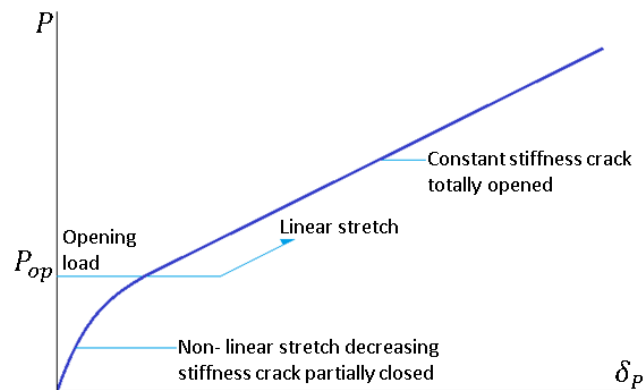


Figure 2. Curve load vs. load application point displacement (P vs. δ_P) with an initial non-linear stretch showing decreasing stiffness until the crack opens at P_{op} , followed by a linear stretch with constant stiffness (adapted from [1]).

Elber identified that this gradual opening behavior is linked to the envelope of tensile residual strains that wraps fatigue cracks, left by the plastic zone that always accompanies them. Crack closure is thus caused by the elastic unloading of residual ligaments, which tend to compress that envelope (thus the crack faces too) while trying to return to their initial state.

With this discovery, Elber also assumed that cracks can only grow by fatigue after totally opened, assuming that FCG rates are not driven by the stress intensity factor range (ΔK), but instead by its part during which the crack is fully opened, the so-called effective stress intensity factor range $\Delta K_{eff} = K_{max} - K_{op}$ if $K_{min} \leq K_{op}$, where K_{op} is the stress intensity factor caused by the opening load P_{op} (otherwise, if $K_{min} > K_{op}$ the crack is fully open the entire cycle, thus $\Delta K_{eff} = K_{max} - K_{min} = \Delta K$). According to the concept of Elber, the basic equation of FCG rate is [2-8]:

$$\frac{da}{dN} = A_e \Delta K_{eff}^{m_e} \quad (2)$$

With A_e and m_e , as material constants.

1.3 Starting Point

One of the main disagreements between the two theories is whether or not there are thickness effects in the FCG rate, given that the plastic zone sizes depend on the dominant stress state around the crack tip, which in turn depend on the cracked sample thickness. Hence, if K_{op} and ΔK_{eff} depend on the plastic zone, and FCG rate is controlled by ΔK_{eff} , it is logical that thickness affects the FCG. There are published results for and against about the existence of the effect of the thickness in the FCG.

Figure. 3 shows thickness effects on the FCG with three specimens of different thickness, made of Al 2024 T3 alloy. Also, Fig. 4 shows no thickness effect on FCG

rate, with specimens in plane strain state ($t = 25 \text{ mm}$) and specimens in plane stress state ($t = 2 \text{ mm}$), made of AL 7075 T7351 alloy [1-9-10-11-12].

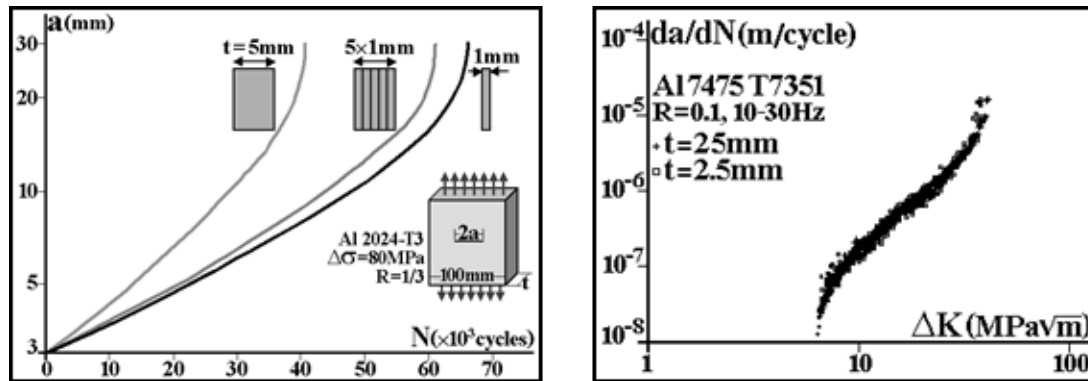


Figure 3. Data showing thickness effects on FCG [11]. Fig. 1. Data showing no thickness effect on da/dN [10].

Moreover, the standard FCG procedures are not thickness-dependent but ASTM E647 only recommends that, if possible, da/dN rates should be measured in specimens as thick as the component the data is intended for [12].

Hence, it was made a series of discriminating FCG tests where crack grew under quasi-constant ΔK loading conditions, in thin and thick specimens of the same material, carefully measuring both the FCG rate and the crack opening load P_{op} while the cracks grew. The specimen thicknesses were chosen to guarantee plane stress conditions in the thin specimens and plane strain conditions in the thicker ones.

2 MATERIALS AND METHODS

Disk Shaped Compact (DC (T)) specimens were selected being made from a single round bar material, which ensure a good chemical homogeneity among them. Besides this, DC (T) specimens were designed to propagate cracks in plane stress and plane strain state, using ASTM standards, with the following equations [1-12-13]:

$$K = \frac{P}{t\sqrt{w}} * \frac{\left(2 + \frac{a}{w}\right) \left[0.76 + 4.8 \frac{a}{w} - 11.58 \left(\frac{a}{w}\right)^2 + 11.43 \left(\frac{a}{w}\right)^3 - 4.08 \left(\frac{a}{w}\right)^4\right]}{\left(1 - \frac{a}{w}\right)^{\frac{3}{2}}} \quad (3)$$

$$z p_{max} = \frac{K_{max}^2}{\pi S_y^2} \begin{cases} t \leq z p_{max} ; \text{plane stress} \\ t > 2.5 \left(\frac{K_{max}}{S_y}\right)^2 \text{plane strain} \end{cases} \quad (4)$$

$$\Delta K_{th} < \Delta K \text{ and } K_{max} \ll K_C \quad (5)$$

$$\Delta K = K_{max} - K_{min} \quad (6)$$

$$R = \frac{K_{min}}{K_{max}} \quad (7)$$

Where: K = stress intensity factor; P = applied force; t = specimen thickness; w = specimen width; a = crack size; $z p_{max}$ = maximum plastic zone (Irwin's estimate) [1]; S_y = tensile strength, yield; K_{max} = stress intensity factor maximum; ΔK = range of stress intensity factor; K_{min} = stress intensity factor minimum; R = Load ratio.

Making the iterative process with these equations, the results of the specimens parameters are in **Figure. 5**.

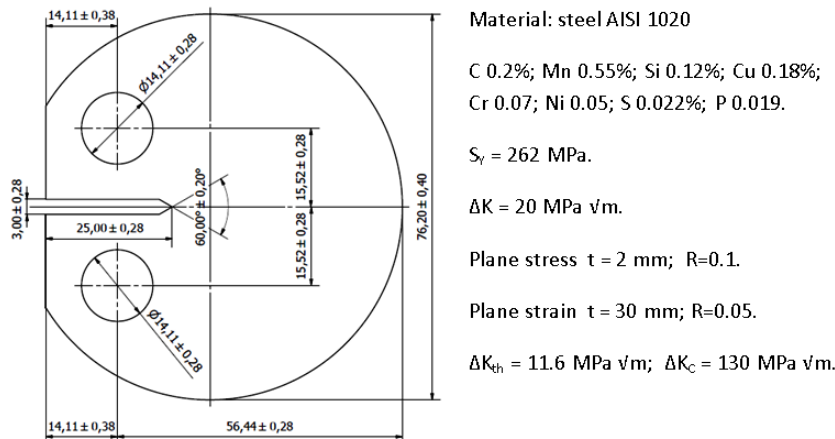


Figure. 5. Disk-Shaped Compact DC(T) specimen, size and material properties.

The tensile strength yield of material was measured in a tensile test. The ΔK_{th} and K_C were taken from the literature [1-14-15], and the chemical composition is supplier information. Besides this, there are also experimental limitations implicit in the calculations (fabricability, assembly on the testing machine...etc.). Tests were conducted on a servohydraulic fatigue testing machine INSTRON 8501 [16]. Strain was measured using a Strain-Gage bonded on the back face of the specimen and seven Strain-Gages located on the crack growth path. Finally crack growth was monitored using a microscope mounted on a micrometric table. **Figure. 6** and Fig. 7, shows the assembly in the machine, of the specimen of 30 mm and of the specimen of 2 mm respectively.



Figure. 6. Assembly plane strain specimen, $t = 30$ mm



Figure 7. Assembly plane stress specimen, $t = 2$ mm.

Stiffness data acquisition was done with a software developed in Labview along with a NI cDAQ-9172 module, which allows to plot the force measurements of the machine load cell (NI 9215 module) with the strain of the eight strain-gages bonded on the specimen (NI 9235 module) [17]. To determine the crack opening load with these data, was developed a program in Matlab with the ASTM method (Opening Force by the Compliance Offset Method), and the classic method of drawing a line in

the linear part of the stiffness curve by least squares. **Figure 8** shows the screen of the program, for calculating of the crack opening load [1-8-12].

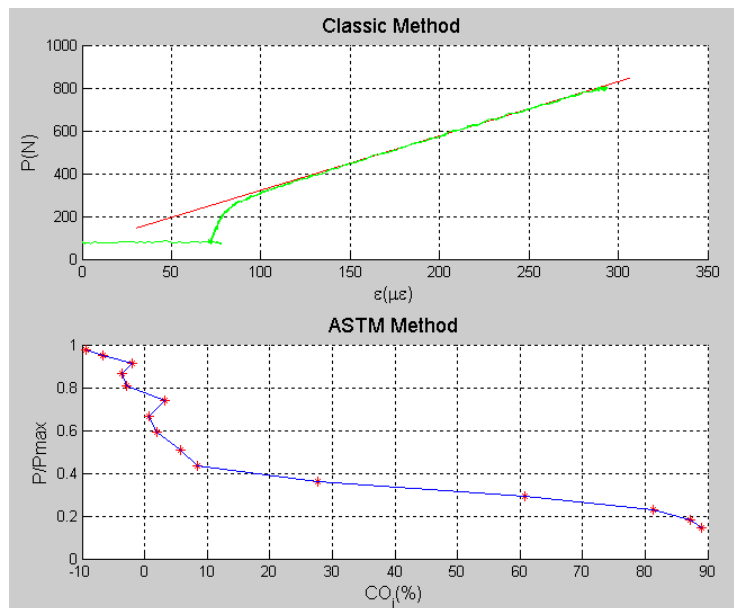


Figure 8. Screen of the crack opening load measurement program.

To calculate the experimental FCG rate, it was used equation of ASTM standard [12]:

$$\frac{da}{dN} = \frac{a_{i+1} - a_i}{N_{i+1} - N_i} \quad (8)$$

Where $(a_{i+1} - a_i)$ is the increment of the crack size regarding the increment of the number of load cycles $(N_{i+1} - N_i)$.

3 RESULTS

The crack opening load P_{op} measured from the various Strain-Gages showed no discrepancy, meaning that the same value was obtained from the near and the far-field strain signals in all experiments. **Figure.** shows an example of a real measurement of P_{op} made with the Strain-Gages, one on the back face and the other one near the crack tip.

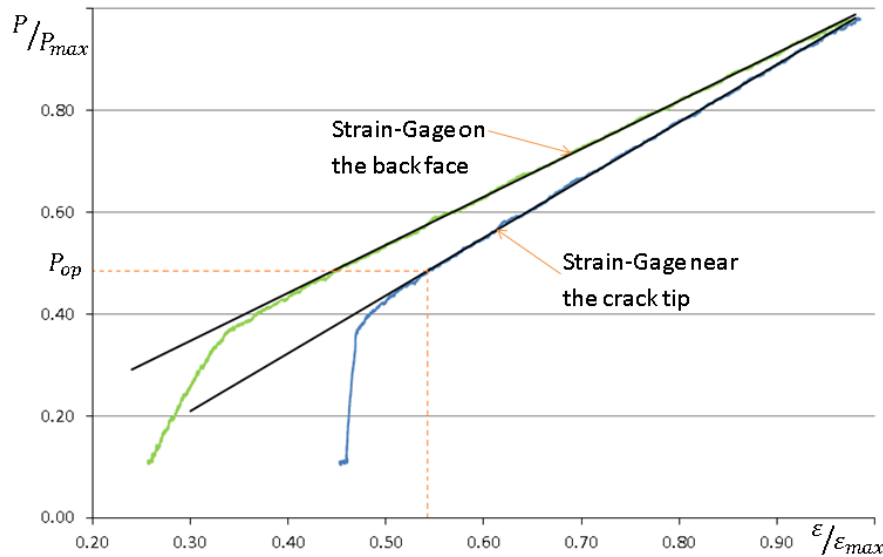


Figure 9: Real measurement of P_{op} made with the Strain-Gages, one on the back face and one near the crack tip.

Figure 10 and **Figure 11** shows the results (da/dN and K_{op} / K_{max} , versus a/w) of the first test in plane strain state (30 mm of thickness and $R=0.05$) and in plane stress state (2mm of thickness and $R=0.1$), respectively. The tests were made with an almost constant ΔK of 20 MPa \sqrt{m} , changing the applied force, according with the crack growth measured with the microscope, with steps $\Delta a \leq 0.1$ mm. The eight strain-gages showed almost the same crack opening load between them.

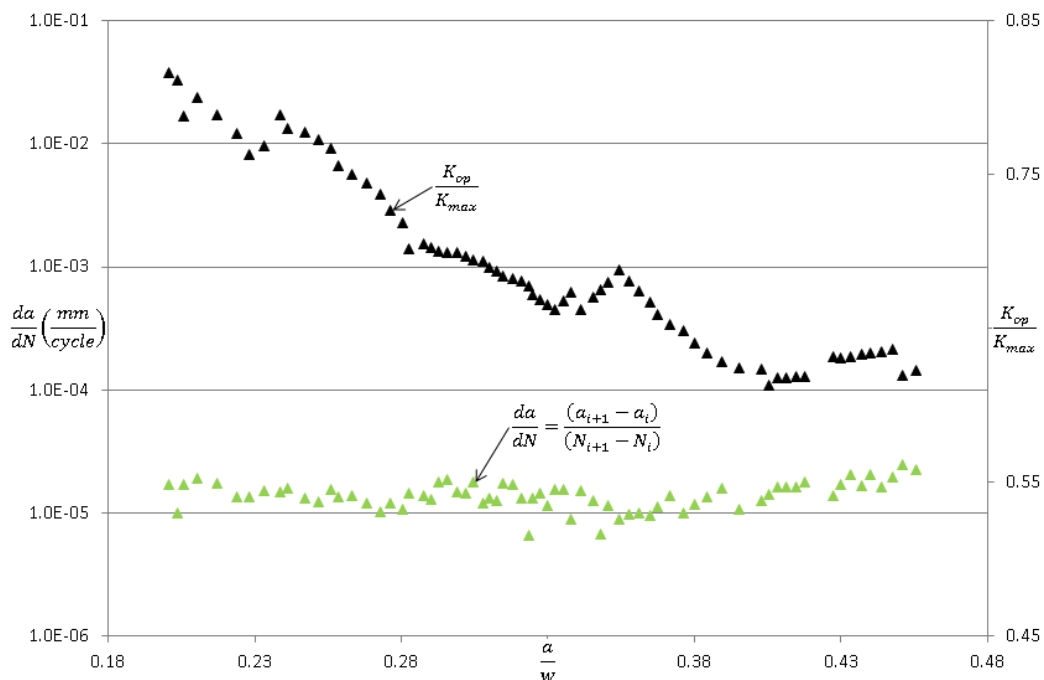


Figure 10. : Data from the FCG test, with ΔK ($R=0.05$) almost constant in plane strain, with the 30 mm thickness specimen, first stage ($1^\circ T$).

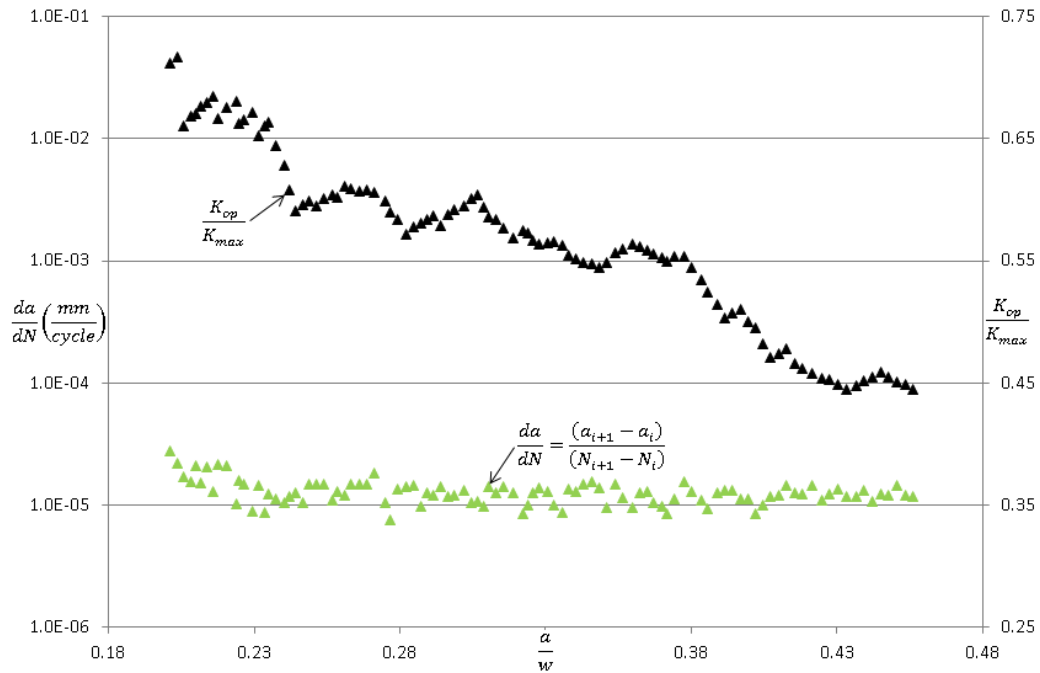


Figure. 11. Data from the FCG test, with ΔK ($R=0.1$) almost constant in plane stress, with the 2 mm thickness specimen, first stage ($1^{\circ}T$).

The first stage of experiments shows that the behavior of the relationship K_{Op} / K_{max} is not consistent with almost constant FCG rate. Then, in order to have a higher reliability, tests were repeated allowing crack reaching a final a/w higher. Now, to make a better comparison between both results, the first ($1^{\circ}T$) and second ($2^{\circ}T$) stage of tests, were mixed in a single figure, for the two types of specimens. **Figure. 12** and **Figure. 13**, show the results of both, FCG rate (da/dN) and K_{Op} / K_{max} data, versus a/w , for the two specimens of 30 mm and the two specimens of 2 mm respectively.

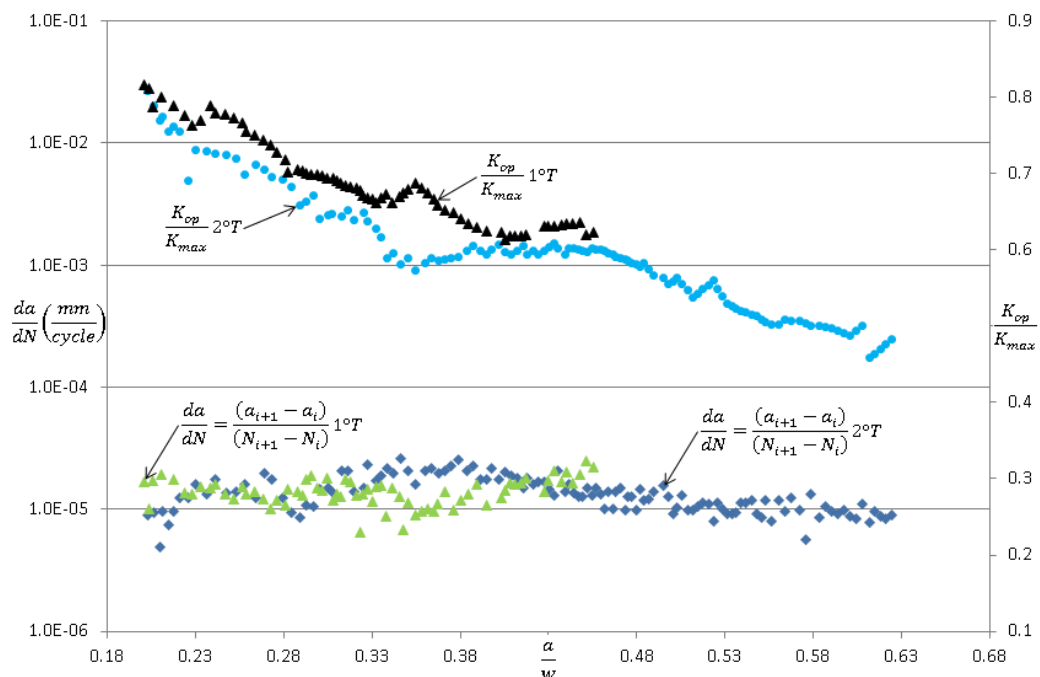


Figure. 12. Data from the FCG experiments, with ΔK ($R=0.05$) almost constant in plane strain, with the 30 mm thickness specimens, of the first stage ($1^{\circ}T$) and second stage ($2^{\circ}T$) of tests.

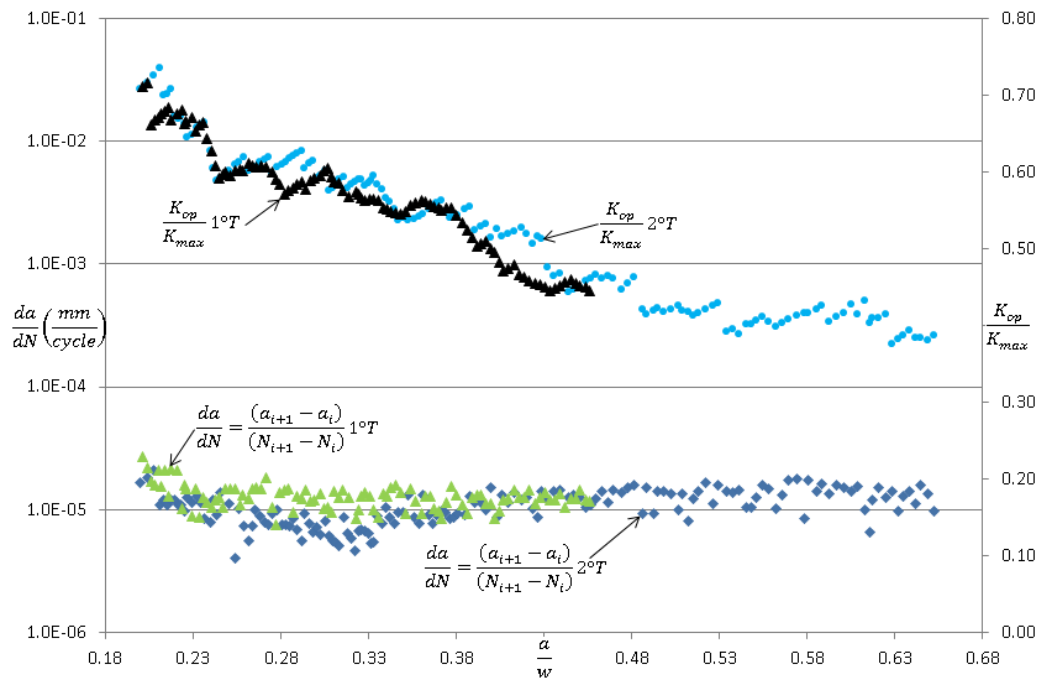


Figure. 13. Data from the FCG experiments, with ΔK ($R=0.1$) almost constant in plane stress, with the 2 mm thickness specimens, of the first stage ($1^\circ T$) and second stage ($2^\circ T$) of tests.

3.1 Discussion

Some authors state that there are differences between crack opening load measure in the field near the crack tip and using a Strain-Gage bonded on the back face of the specimen [18]. However, performed experiments showed approximately the same crack opening load measure by the two ways. Also, the tests show at almost constant ΔK , reproduce the principle of the Paris' theory: cracks of different lengths subjected to the same nominal ΔK will advance by equal increments of crack extension per cycle (Equation 1) [1-12].

Obtained results did not show any thickness effect in the FCG rate. The average in all experiments was approximately 1.3×10^{-5} mm/cycle. This agrees with results shown in Fig. 4 and with authors that neglect thickness effects [12,19-21].

Moreover, the decline of the relationship K_{op}/K_{max} , while the crack was growing, shows that Elber's theory does not describe the behavior of the tests with FCG almost constant, considering that the FCG rate predicts with the equation 2, only can be constant if ΔK_{eff} is fixed [1-8-22].

Finally, the repeatability of the tests was satisfactory, given that the FCG rate and the behavior of the relationship K_{op}/K_{max} of the first stage, was reproduced in the second stage of experiments.

4. CONCLUSIONS

It was shown that sample's thickness had no effect on the experimental results of the FCG rate, since the arithmetic average, of the plane stress specimens (2 mm) and of the plane strain specimens (30mm), is approximately the same (1.3×10^{-5} mm/cycle). The principle of the Paris' theory; cracks of differing lengths subjected to the same nominal ΔK and K_{max} will advance by equal increments of crack extension per cycle, describes successfully the experiments made in this work, indicating that ΔK is the driving force in this tests.

The fact that K_{op}/K_{max} fall as the crack growths and the thickness do not have any effect in the tests shows that the Elber's theory does not describe the FCG rate of the experiments performed in this paper.

REFERENCES

- 1 Castro JTP, Meggiolaro MA. Fadiga - Técnicas e Práticas de Dimensionamento Estrutural sob Cargas Reais de Serviço. Scotts Valley: CreateSpace; 2009.
- 2 Schijve J. Fatigue of Structures and Materials, 2nd Ed. Delft: Springer; 2009.
- 3 Dowling NE. Mechanical Behavior of Materials, 3rd Ed. New Jersey: Prentice Hall; 2007.
- 4 Skorupa M. Load Interaction Effects During Fatigue Crack Growth Under Variable Amplitude Loading - a Literature Review - Part II: Qualitative Interpretation. Fatigue and Fracture of Engineering Materials and Structures 1999; 22: 905-926.
- 5 Kemp PMJ. Fatigue Crack Closure – a Review. Technical Report TR90046, Royal Aerospace Establishment. 1990.
- 6 Paris PC, Erdogan F. A Critical Analysis of Crack Propagation Laws. Journal of Basic Engineering. 1963; 85: 528-534.
- 7 Elber W. Fatigue Crack Closure Under Cyclic Tension. Engineering fracture mechanics. 1970; 2: 37-45.
- 8 Elber W. The Significance of Fatigue Crack Closure. Damage Tolerance of Aircraft Structures. 1971; 486: 230-242.
- 9 Mills WJ, Hertzberg RW. The Effect of Sheet Thickness on Fatigue Crack Retardation in 2024-T3 Aluminum Alloy. Engineering Fracture Mechanics. 1975; 7:705-711.
- 10 Ruckert COFT, Tarpani JR, Milan MT., Bose WWF, Spinell D. Evaluating the Berkovitz Method to Predict Fatigue Loads in Mechanical Failure Investigations. Journal of Materials Engineering and Performance. 2006; 15: 661-667.
- 11 Matsuura S, Tanaka K. The Influence of Sheet Thickness on Delayed Retardation Phenomena in Fatigue Crack Growth in HT80 Steel and A5083 Aluminum Alloy. Engineering Fracture Mechanics. 1980; 13: 293-306.
- 12 ASTM E647. Standard Test Methods for Measurement of Fatigue Crack Growth Rates. ASTM Standards. 2013; 03.01.
- 13 ASTM E399. Standard Test Method for Linear-Elastic Plane-Strain Fracture Toughness K_{Ic} of Metallic Materials 2013; 03.01.
- 14 Material Property Data [internet site]. MatWeb [access 10 Jan. 2013]. Available in: <http://www.matweb.com>.
- 15 Aços especiais [internet site]. Tenax [access 10 January 2013]. Available in: <http://www.tenax.com.br>.
- 16 INSTRON. [internet site]. [access 8 November 2013]. Available in: <http://www.instron.com>
- 17 National Instruments. [internet site]. [access 15 February 2013]. Available in: <http://www.ni.com>.
- 18 Skorupa M, Machniewicz T, Skorupa A. Applicability of the ASTM Compliance Offset Method to Determine Crack Closure Levels for Structural Steel. International Journal of Fatigue. 2007; 29: 1434–1451.
- 19 Vasudevan AK, Sadananda K, Louat N. Reconsideration of Fatigue Crack Closure. Scripta Metallurgica et Materialia. 1992; 27: 1663-1678.
- 20 Vasudevan AK, Sadananda K, Holtz RL. Unified Approach to Fatigue Damage Evaluation. NRL Review. 2003: 51-57.
- 21 Vasudevan AK, Sadananda K, Holtz RL. Analysis of vacuum fatigue crack growth results and its implications. International Journal of Fatigue. 2005; 27: 1519-1529,
- 22 NASGRO. Fracture Mechanics and Fatigue Crack Growth Analysis Software. Reference Manual. NASA. 2002. Version 4.02.